JACS
JOURNAL OF THE AMERICAN CHEMICAL SOCIETY

Communication

pubs.acs.org/JACS

Light-Driven, Proton-Controlled, Catalytic Aerobic C−H Oxidation Mediated by a Mn(III) Porphyrinoid Complex

Heather M. Neu,[†] Jieun Jung,[‡] Regina A. Baglia,[†] Maxime A. Siegler,[†] Kei Ohkubo,[‡] Shunichi Fukuzumi,*[,‡,§] and David P. Goldberg*[,†]

[†]Department of Chemistry, The Johns Hopkins University, Baltimore, Maryland 21218, United States

[‡]Department of Material and Life Science, Graduate School of Engineering, Osaka University, ALCA, Japan Science and Technology Agency, Suita, Osaka 565-0871, Japan

[§]Department of Bioinspired Science, Ewha Womans University, Seoul 120-750, Korea

Supporting Information

ABSTRACT: The visible light-driven, catalytic aerobic oxidation of benzylic C−H bonds was mediated by a Mn^{III} corrolazine complex. To achieve catalytic turnovers, a strict selective requirement for the addition of protons was established. The resting state of the catalyst was unambiguously characterized by X-ray diffraction as $[Mn^{III}(H_2O)(TBP_8Cz(H))]^+$, in which a single, remote site on the ligand is protonated. If two remote sites are protonated, however, reactivity with O_2 is shut down. Spectroscopic methods revealed that the related $Mn^V(O)$ complex is also protonated at the same remote site at −60 °C, but undergoes valence tautomerization upon warming.

The activation of molecular oxygen is a critical transformation in biology, which is mediated by both heme and nonheme metal centers.[1] Synthetic, biomimetic transition metal complexes aimed at activating O_2 have been targeted by employing both porphyrinoid and nonheme polydentate ligands, and some of these efforts have resulted in important mechanistic insights and catalysts for the oxygenation of a range of organic substrates.[2] The catalytic, aerobic oxidation of C−H bonds with first-row, biologically relevant metal complexes remains a particularly important, yet challenging goal.[3] Although some Fe and Mn metalloporphyrins, and related metallomacrocycles (e.g., phthalocyanines), can catalyze the oxidation of C−H bonds with O_2, drawbacks remain in most cases. Such drawbacks include the need for stoichiometric coreductants, and the involvement of poorly controlled radical-type pathways.[2j,3] The mechanisms of these systems, including the role of high-valent metal-oxo species, is often poorly understood.

Corroles are modified porphyrinoid ligands that stabilize high-valent metal-oxo species and can exhibit catalytic activity different from their porphyrin analogs. A Cr^{III} corrole catalyzes the aerobic oxidation of PPh_3 via a $Cr^V(O)$ intermediate.[4] Under visible light irradiation, diiron(IV) μ-oxo biscorroles have been shown to catalyze the aerobic oxidation of phosphine and C−H substrates, presumably through a disproportionation pathway that involves μ-oxo-bridge cleavage and leads to formation of $Fe^{III}/Fe^V(O)$ intermediates.[5] Diiron(III)-μ-oxo-bridged porphyrins also mediate photoactivated aerobic oxidations through similar μ-oxo cleavage mechanisms.[6]

In previous work, we showed that a stable $Mn^V(O)$ complex prepared with a corrolazine ligand, which is a *meso-N*-substituted analog of a corrole, could be synthesized via photoirradiation of a Mn^{III} precursor, O_2 (or air), and C−H substrates.[7a] This work was the first example of the synthesis of a $Mn^V(O)$ complex from air, light, and a proton/electron source.[7a] The addition of toluene derivatives to the Mn^{III}/light/O_2 system led to selective C−H hydroxylation of benzylic C−H bonds.[7b] However, the inherent stability of the $Mn^V(O)$ complex toward the toluene derivatives limited this chemistry to a strictly stoichiometric process. Only in the case of PPh_3, or dihydroacridine, which has a very weak C−H bond (BDFE = 69 kcal mol^{-1}), was catalytic turnover obtained.[7,8]

Herein we report the visible light-driven, catalytic aerobic oxidation of benzylic C−H bonds via the proton-controlled activation of a Mn^{III} corrolazine complex. The selective addition of a strong proton donor leads to the formation of new mono- and diprotonated Mn^{III} complexes, which were characterized by single crystal X-ray diffraction (XRD). The monoprotonated complex is capable of reacting with air, light, and benzylic C−H bonds to give a high-valent Mn−oxo complex. Under the right conditions, the controlled addition of protons provides access to a catalytic cycle. Low-temperature methods were used to trap a novel, proton-activated form of the $Mn^V(O)$ complex which may play a role in the catalytic cycle.

Previously it was shown that photoirradiation ($\lambda > 400$ nm) of $Mn^{III}(TBP_8Cz)$ (TBP_8Cz = octakis(*p-tert*-butylphenyl corrolazinato^{3-}) in the presence of excess O_2 and hexamethylbenzene (HMB) in benzonitrile (PhCN) led to the selective oxidation of HMB to pentamethylbenzyl alcohol (PMB−OH) (87%) with clean formation of $Mn^V(O)(TBP_8Cz)$.[7b] This $Mn^V(O)$ complex oxidizes relatively weak C−H bonds such as those found in dihydroanthracene (BDFE = 76 kcal mol^{-1}), but is essentially unreactive toward stronger C−H bonds such as those found in toluene (BDFE = 87 kcal mol^{-1}) or its derivatives.[8] The selective hydroxylation of HMB was therefore limited to strictly stoichiometric reactivity.[7b] We speculated that addition of a strong proton donor might activate the $Mn^V(O)$ complex toward oxidation of the stronger C−H bonds found in HMB, providing entry into a *catalytic* oxidation pathway.

Received: January 24, 2015
Published: April 3, 2015

DOI: 10.1021/jacs.5b00816
J. Am. Chem. Soc. 2015, 137, 4614−4617

Addition of the strong proton donor $[H(OEt_2)_2]^+[B(C_6F_5)_4]^-$ ($H^+[B(C_6F_5)_4]^-$) to $Mn^{III}(TBP_8Cz)$ in benzene (C_6H_6) caused an immediate color change of the brown Mn^{III} complex to a brown-red solution. The addition of excess HMB (1000 equiv) under ambient conditions to this solution, followed by photoirradiation with visible light (λ > 400 nm), led to the slow bleaching of the solution over 5.5 h. Monitoring of this reaction by UV−vis confirmed the slow decay of the protonated Mn^{III} complex, which exhibited distinct Soret and Q-bands at 446 and 728 nm (Figure S3). Analysis of the reaction mixture by GC-FID revealed the production of PMB−OH and the corresponding aldehyde PMB−CHO (Scheme 1) with 18 turnovers for

Scheme 1

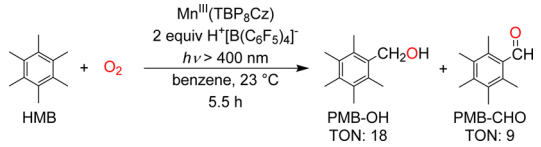

PMB−OH and 9 turnovers for PMB−CHO. Both oxidation products increase steadily over time, and catalytic activity appears only limited by catalyst stability. In the absence of light, O_2, or Mn^{III} complex, no oxidized products were detected. As anticipated, the addition of H^+ to the Mn catalyst leads to the catalytic oxidation of HMB with only air and light as additives.

The independent reaction of $Mn^{III}(TBP_8Cz)$ with $H^+[B(C_6F_5)_4]^-$ was investigated to determine the effect of H^+ on the Mn^{III} complex. These independent experiments were initially run in CH_2Cl_2, as opposed to C_6H_6, because of the available UV−vis data on Mn corrolazine complexes in CH_2Cl_2.[9,10] The starting Mn^{III} complex (435, 685 nm) was converted to a new brown-red species upon addition of 1 equiv of $H^+[B(C_6F_5)_4]^-$ (446, 730 nm) (Figure 1). This new spectrum (446, 730 nm) was almost

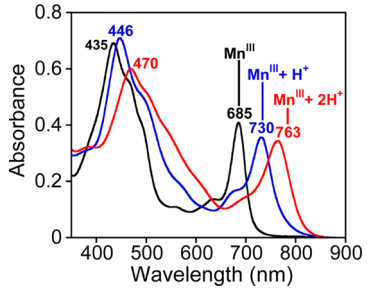

Figure 1. UV−vis spectral changes for $Mn^{III}(TBP_8Cz)$ (12 μM, black line) upon addition of 1 equiv (blue line) and 2 equiv (red line) of $H^+[B(C_6F_5)_4]^-$ in CH_2Cl_2 (2 mL) at 25 °C.

identical to that seen for the resting state of the catalyst in C_6H_6. Introduction of a second equivalent of H^+ caused a further change to a second species with further red-shifted Soret and Q-bands at 470 and 763 nm. Spectral titrations (Figure S4) showed that no further changes occur upon addition of up to 5 equiv of H^+. Similar spectra were obtained in dry C_6H_6 (Figure S10).

The UV−vis data in Figure 1 clearly show that there are two distinct species accessible via protonation of the starting Mn^{III} corrolazine. The three Mn^{III} complexes identified in Figure 1 were successfully crystallized and unambiguously characterized by XRD. The crystal structures of the neutral, mono- and diprotonated Mn^{III} derivatives are presented in Figure 2. The structure of the neutral Mn^{III} complex contains a five-coordinate Mn^{III} ion with a water ligand located in the axial position, similar to the structure of a MeOH-bound $Mn^{III}(MeOH)(TBP_8Cz)$.[9b] The axial H_2O ligands of two adjacent metallocorrolazines are H-bond donors to the meso-N atoms of the neighboring Cz ligand via a set of 1 + 1 O−H···N hydrogen bonds (i.e., only one H-bond per axial H_2O ligand), resulting in H-bonded dimers of $Mn^{III}(H_2O)$ complexes in the solid state. Treatment of the starting Mn^{III} complex with 1 equiv of $H^+[B(C_6F_5)_4]^-$ in CH_2Cl_2, followed by removal of solvent and recrystallization from toluene/heptane, led to dark brown crystals of $[Mn^{III}(H_2O)(TBP_8Cz(H))][B(C_6F_5)_4]$. The crystal structure reveals that monoprotonation most likely occurs at one of the meso-N atoms (N1(H)) adjacent to the direct pyrrole−pyrrole bond of the Cz ligand. The axial H_2O ligand seen in the neutral Mn^{III} starting complex and H-bonded dimers are retained. Dissolution of crystalline $[Mn^{III}(H_2O)(TBP_8Cz(H))][B(C_6F_5)_4]$ yields the same UV−vis spectrum as seen for the in situ protonation of the Mn^{III} complex via addition of 1 equiv of $H^+[B(C_6F_5)_4]^-$ (λ_{max} = 446, 730 nm) (Figure S6). If 2 equiv of $H^+[B(C_6F_5)_4]^-$ are added to the neutral Mn^{III} complex, a new complex in the form of dark brown crystals can be isolated. XRD analysis shows that this new species is doubly protonated with the molecular formula $[Mn^{III}(H_2O)(TBP_8Cz(H)_2)][B(C_6F_5)_4]_2$ (Figure 2). Both H-atoms were unambiguously located on the opposite meso-N atoms (N1 and N5) (Figure S2). Unlike the neutral and monoprotonated structures, this complex exhibits no H-bonding to nearest neighbors and crystallizes in isolated molecular units. The UV−vis spectrum of crystalline $[Mn^{III}(H_2O)(TBP_8Cz(H)_2)][B(C_6F_5)_4]_2$ redissolved in CH_2Cl_2 matches that seen for the in situ diprotonation of the Mn^{III} complex following treatment with 2 equiv of H^+ (λ_{max} = 470, 763 nm) (Figure S8). The metrical parameters for each of the structures show little variation upon mono- and diprotonation, with the exception of a slight shortening (Δd(Mn−O) = 0.028(3) Å) of the Mn^{III}−OH_2 distance.

The preparation of crystalline mono- and diprotonated Mn^{III} complexes provided pure material for testing as possible catalysts in the observed light-driven, aerobic C−H oxidation. Monoprotonated $[Mn^{III}(H_2O)(TBP_8Cz(H))][B(C_6F_5)_4]$ was dissolved in CH_2Cl_2 or C_6H_6 with excess HMB (1000 equiv) under aerobic conditions. Photoirradiation of this solution for 30 min at 23 °C followed by analysis by GC-FID showed both alcohol and aldehyde products were formed, but only in stoichiometric amounts (PMB−OH: TON = 0.4; PMB−CHO: TON = 0.7); i.e., no catalysis was observed. Monitoring this reaction by UV−vis showed isosbestic conversion of the spectrum for $[Mn^{III}(H_2O)(TBP_8Cz(H))]^+$ to a new spectrum with features at 418 and 784 nm. This new spectrum (Figure S12) matches that seen previously for the Mn^{IV}-oxo π-radical cation complex $[Mn^{IV}(O)(TBP_8Cz^{\bullet+})(LA)]^+$ (LA = Lewis acid = Zn^{II}, B$(C_6F_5)_3$), a valence tautomer of $Mn^{V}(O)(TBP_8Cz)$ stabilized by Lewis acids.[10] In support of this analysis, reaction of crystalline $[Mn^{III}(H_2O)(TBP_8Cz(H))][B(C_6F_5)_4]$ with the O-atom donor PhIO leads to isosbestic conversion to $[Mn^{IV}(O)(TBP_8Cz^{\bullet+})(H)]^+$ (Figure S13), instead of $Mn^{V}(O)(TBP_8Cz)$, which is the major product from $[Mn^{III}(H_2O)(TBP_8Cz)]$ + PhIO.[9b] These results indicate that generation of the valence tautomer $[Mn^{IV}(O)(TBP_8Cz^{\bullet+})(H)]^+$ occurs if 1 equiv of H^+ is employed.

The use of crystalline *diprotonated* $[Mn^{III}(H_2O)(TBP_8Cz(H)_2)][B(C_6F_5)_4]_2$ as starting material, in contrast, leads to catalytic turnover in the light-driven oxidation of HMB, giving PMB−OH (TON = 16) and PMB−CHO (TON = 11) after 5 h in C_6H_6 at 23 °C. However, the initial spectrum for the

DOI: 10.1021/jacs.5b00816
J. Am. Chem. Soc. 2015, 137, 4614−4617

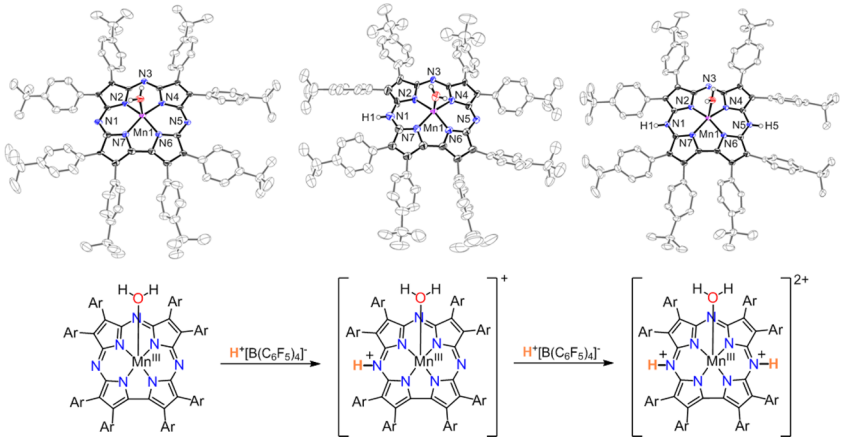

Figure 2. (Top) Displacement ellipsoid plots (50% probability level) for $Mn^{III}(TBP_8Cz)(H_2O)$ (left), $[Mn^{III}(H_2O)(TBP_8Cz(H))]^+$ (center), and $[Mn^{III}(H_2O)(TBP_8Cz(H)_2)]^{2+}$ (right) at 110(2) K. (Bottom) Addition of 1 and 2 equiv of $H^+[B(C_6F_5)_4]^-$ to $Mn^{III}(TBP_8Cz)$.

diprotonated complex (470, 763 nm) rapidly (≤2 min) converts to a spectrum characteristic of the *monoprotonated* Mn^{III} *species* (446, 728 nm) under catalytic conditions, and no evidence for the formation of either the $Mn^V(O)$ or $Mn^{IV}(O)(\pi$-radical cation) (Figure S14). The spectrum for the diprotonated Mn^{III} complex can be maintained if a third equivalent of $H^+[B(C_6F_5)_4]^-$ is added prior to photoirradiation, but under these conditions no oxidation products of HMB were obtained. Taken together, these observations indicate that the presence of 2 equiv of H^+ are required for catalytic turnover, and it is the monoprotonated Mn^{III} complex that is the catalytically active resting state.

Further insight regarding the role of 2 equiv of H^+ came from examining the diprotonated Mn^{III} complex in "wet" C_6H_6 under aerobic conditions, versus dry C_6H_6 under an inert atmosphere. It was found that residual H_2O, present under aerobic conditions, acted as a weak base and led to the deprotonation of $[Mn^{III}(H_2O)(TBP_8Cz(H)_2)]^{2+}$ to give the monoprotonated complex, while under strictly anaerobic conditions (doubly distilled C_6H_6, inert atmosphere), the diprotonated complex was observed (Figures S9–S11). Thus, the monoprotonated Mn^{III} complex is formed under the aerobic conditions of the catalytic reaction.

The data presented herein, together with previous femtosecond transient absorption measurements,[7b] lead to the proposed catalytic cycle shown in Scheme 2. The monoprotonated Mn^{III} complex is the resting state of the catalyst, which is activated by photoexcitation to a tripquintet excited state ($^5T_1$) that rapidly converts to the O_2-reactive tripseptet ($^7T_1$) excited state. Entry of O_2 gives a putative Mn^{IV}(superoxo) complex, which can either undergo rapid back electron transfer to the ground state and release of O_2 or can abstract an H-atom from the HMB substrate. The resulting $Mn^{IV}(OOH)$ complex can then hydroxylate the HMB radical via O–O cleavage and rebound of $OH^•$, to yield PMB–OH and the $Mn^V(O)$ complex. The $Mn^V(O)$ complex is activated in the presence of acid under the catalytic conditions, leading to oxidation of HMB (or PMB–OH) and completing the catalytic cycle.

Attempts were made to gain insights into the final step of the catalytic cycle by reacting isolated $Mn^V(O)(TBP_8Cz)$ with $H^+[B(C_6F_5)_4]^-$ in CH_2Cl_2 or benzene. This reaction, when run with 1 equiv of H^+ at 23 °C, afforded the valence tautomer $[Mn^{IV}(O)(TBP_8Cz^{•+})(H)]^+$ (Scheme S1, Figure S15). This species was unreactive toward either excess HMB or PMBOH (1000 equiv) for up to 2 h at 23 °C, and photoirradiation of this

Scheme 2. Proposed Catalytic Cycle for the Oxidation of HMB

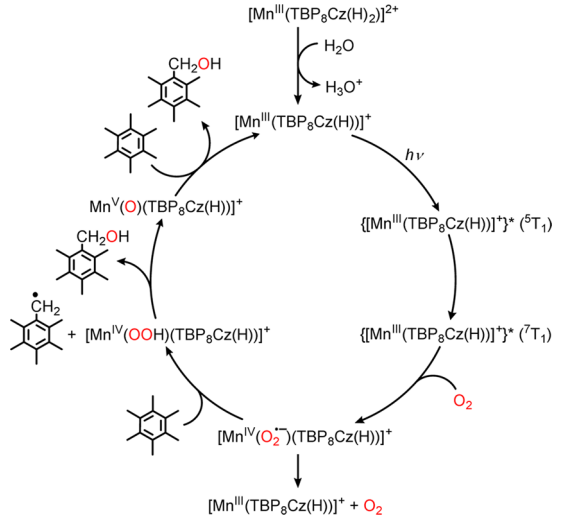

solution caused significant decomposition (~40% bleaching). The addition of 2 equiv of $H^+[B(C_6F_5)_4]^-$ to isolated $Mn^V(O)(TBP_8Cz)$ in the presence of light and excess HMB caused rapid (<10 s) formation of Mn^{III}, although organic oxidation products could not be identified. The exact nature of the catalytically active intermediate cannot be assigned, but it is clear that 2 equiv of H^+ rapidly destabilize the isolated $Mn^V(O)$ complex, and these observations suggest that H^+ may assist in activating the $Mn^V(O)$ complex to induce turnover under the appropriate catalytic conditions.

Further examination of the reaction of $Mn^V(O)(TBP_8Cz)$ and $H^+[B(C_6F_5)_4]^-$ at low temperature (−60 °C) led to an isosbestic change together with the formation of a distinct, new species with λ_{max} = 436, 650 nm (Figure S16). This spectral change is reversible upon addition of 1 equiv of 1,8-bis(dimethylamino)-naphthalene (proton sponge), consistent with an acid–base transformation (Figure S17). The structure of the new Mn^V species (436, 650 nm) was characterized by low-temperature 1D and 2D NMR spectroscopy. The ^1H NMR spectra (−50 to −60 °C) of the starting $Mn^V(O)$ complex and the monoprotonated derivative are compared in Figure 3. Both spectra are diamagnetic, confirming that the low-spin (d^2) Mn^V oxidation state is retained at −60 °C (Figure 3). The most notable difference between the two species is the appearance of a new

DOI: 10.1021/jacs.5b00816
J. Am. Chem. Soc. 2015, 137, 4614–4617

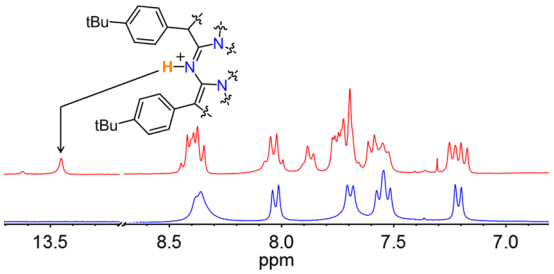

Figure 3. Comparison of ^{1}H NMR spectra (aryl region) for $[Mn^V(O)(TBP_8Cz(H))]^+$ (red) at −60 °C and $Mn^V(O)(TBP_8Cz)$ (blue) at −50 °C.

peak at 13.45 ppm following addition of the $H^+[B(C_6F_5)_4]^-$. The chemical shift of this resonance is consistent with protonation of a meso-N atom, as seen for the Mn^{III} complexes, and is shifted downfield due to a ring current effect. This new peak disappeared upon exchange with D_2O, while the other peaks remained intact (Figure S21). The protonated complex also exhibits a new multiplet at 7.87 ppm, along with additional splitting in both the aromatic and ^{t}Bu regions (Figures S20). These perturbations are consistent with a lowering of the molecular symmetry, as expected for protonation at a single meso-N position adjacent to the direct pyrrole−pyrrole bond of the Cz ligand. Definitive assignment of the 13.45 ppm peak comes from ^{1}H−^{1}H 2D nuclear Overhauser effect spectroscopy (NOESY) (Figure S22). Well-defined cross-peaks are observed between the new peak at 13.45 ppm and peaks at 8.04 and 7.70 ppm, indicating an interaction between the meso N−H and two nearby (<5 Å) aryl C−H resonances. From the ^{1}H−^{1}H 2D correlation (COSY) spectrum, we can clearly assign the aryl C−H resonances at 8.04 and 7.70 ppm as arising from protons on separate benzene rings (Figure S23). Taken together, the NMR data show that a meso-N atom closest to the direct pyrrole−pyrrole bond is protonated upon addition of $H^+[B(C_6F_5)_4]^-$ to the $Mn^V(O)$ complex at −60 °C (Scheme S1). Thus, the $Mn^V(O)$ complex can be protonated at the meso-N position as seen for Mn^{III}, and this protonation site, together with possible protonation at the oxo position, may play a role in the proton-assisted, light-driven, catalytic aerobic oxidation of HMB.

In summary we have shown that a Mn^{III} porphyrinoid complex can catalyze the visible light-driven, aerobic oxidation of benzylic C−H bonds. Strict control of the proton content is necessary to achieve catalytic turnover. The Mn^{III} resting state of the catalyst was definitively characterized by XRD. Low temperature spectroscopic methods have identified a new form of a $Mn^V(O)$ corrolazine, in which a remote site is selectively protonated, and suggest a potential binding site for H^+ along the catalytic pathway. Although we cannot definitively characterize the precise protonation state of the Mn^V complex under catalytic conditions, taken together, the data indicate that 2 equiv of acid are necessary for catalysis. This work furthers our knowledge regarding the criteria for developing biomimetic heme complexes for O_2 activation catalysts and suggests a promising strategy in catalyst design that could involve the incorporation of remote ligand sites for modification by noncovalent interactions.

■ ASSOCIATED CONTENT

Ⓢ Supporting Information

CIF, experimental procedures, Scheme S1, Table S1, and Figures S1−S23. This material is available free of charge via the Internet at http://pubs.acs.org.

■ AUTHOR INFORMATION

Corresponding Authors

*dpg@jhu.edu

*fukuzumi@chem.eng.osaka-u.ac.jp

Notes

The authors declare no competing financial interest.

■ ACKNOWLEDGMENTS

This work was supported by the NIH (GM101153) and NSF (CHE121386) to D.P.G. and an ALCA and SENTAN project (to S.F.) from JST, Japan. We thank Prof. K. D. Karlin for instrumentation use, and we thank Dr. A. Majumdar and Dr. J. Tang for helpful NMR discussions.

■ REFERENCES

(1) (a) Sono, M.; Roach, M. P.; Coulter, E. D.; Dawson, J. H. *Chem. Rev.* **1996**, *96*, 2841. (b) Denisov, I. G.; Makris, T. M.; Sligar, S. G.; Schlichting, I. *Chem. Rev.* **2005**, *105*, 2253. (c) Kovaleva, E. G.; Lipscomb, J. D. *Nat. Chem. Biol.* **2008**, *4*, 186.

(2) (a) Ellis, P. E.; Lyons, J. E. *Coord. Chem. Rev.* **1990**, *105*, 181. (b) O'Reilly, M. E.; Del Castillo, T. J.; Falkowski, J. M.; Ramachandran, V.; Pati, M.; Correia, M. C.; Abboud, K. A.; Dalal, N. S.; Richardson, D. E.; Veige, A. S. *J. Am. Chem. Soc.* **2011**, *133*, 13661. (c) Park, Y. J.; Ziller, J. W.; Borovik, A. S. *J. Am. Chem. Soc.* **2011**, *133*, 9258. (d) Jaafar, H.; Vileno, B.; Thibon, A.; Mandon, D. *Dalton Trans.* **2011**, *40*, 92. (e) Lionetti, D.; Day, M. W.; Agapie, T. *Chem. Sci.* **2013**, *4*, 785. (f) de Torres, M.; van Hameren, R.; Nolte, R. J. M.; Rowan, A. E.; Elemans, J. A. A. W. *Chem. Commun.* **2013**, *49*, 10787. (g) Saha, B.; Gupta, D.; Abu-Omar, M. M.; Modak, A.; Bhaumik, A. *J. Catal.* **2013**, *299*, 316. (h) Zhang, Q.; Gorden, J. D.; Goldsmith, C. R. *Inorg. Chem.* **2013**, *52*, 13546. (i) Dai, F.; Yap, G. P. A.; Theopold, K. H. *J. Am. Chem. Soc.* **2013**, *135*, 16774. (j) Sorokin, A. B. *Chem. Rev.* **2013**, *113*, 8152. (k) Ray, K.; Pfaff, F. F.; Wang, B.; Nam, W. *J. Am. Chem. Soc.* **2014**, *136*, 13942.

(3) (a) Grinstaff, M. W.; Hill, M. G.; Labinger, J. A.; Gray, H. B. *Science* **1994**, *264*, 1311. (b) Punniyamurthy, T.; Velusamy, S.; Iqbal. *J. Chem. Rev.* **2005**, *105*, 2329. (c) Roduner, E.; Kaim, W.; Sarkar, B.; Urlacher, V. B.; Pleiss, J.; Gläser, R.; Einicke, W. D.; Sprenger, G. A.; Beifuss, U.; Klemm, E.; Liebner, C.; Hieronymus, H.; Hsu, S. F.; Plietker, B.; Laschat, S. *ChemCatChem* **2013**, *5*, 82.

(4) Mahammed, A.; Gray, H. B.; Meier-Callahan, A. E.; Gross, Z. *J. Am. Chem. Soc.* **2003**, *125*, 1162.

(5) (a) Harischandra, D. N.; Lowery, G.; Zhang, R.; Newcomb, M. *Org. Lett.* **2009**, *11*, 2089. (b) Zhang, R.; Vanover, E.; Chen, T. H.; Thompson, H. *Appl. Catal., A* **2013**, *464*, 95.

(6) Rosenthal, J.; Luckett, T. D.; Hodgkiss, J. M.; Nocera, D. G. *J. Am. Chem. Soc.* **2006**, *128*, 6546.

(7) (a) Prokop, K. A.; Goldberg, D. P. *J. Am. Chem. Soc.* **2012**, *134*, 8014. (b) Jung, J.; Ohkubo, K.; Prokop-Prigge, K. A.; Neu, H. M.; Goldberg, D. P.; Fukuzumi, S. *Inorg. Chem.* **2013**, *52*, 13594. (c) Jung, J.; Ohkubo, K.; Goldberg, D. P.; Fukuzumi, S. *J. Phys. Chem. A* **2014**, *118*, 6223.

(8) Warren, J. J.; Tronic, T. A.; Mayer, J. M. *Chem. Rev.* **2010**, *110*, 6961.

(9) (a) Neu, H. M.; Yang, T. H.; Baglia, R. A.; Yosca, T. H.; Green, M. T.; Quesne, M. G.; de Visser, S. P.; Goldberg, D. P. *J. Am. Chem. Soc.* **2014**, *136*, 13845. (b) Lansky, D. E.; Mandimutsira, B.; Ramdhanie, B.; Clausen, M.; Penner-Hahn, J.; Zvyagin, S. A.; Telser, J.; Krzystek, J.; Zhan, R.; Ou, Z.; Kadish, K. M.; Zakharov, L.; Rheingold, A. L.; Goldberg, D. P. *Inorg. Chem.* **2005**, *44*, 4485.

(10) (a) Leeladee, P.; Baglia, R. A.; Prokop, K. A.; Latifi, R.; de Visser, S. P.; Goldberg, D. P. *J. Am. Chem. Soc.* **2012**, *134*, 10397. (b) Baglia, R. A.; Durr, M.; Ivanovic-Burmazovic, I.; Goldberg, D. P. *Inorg. Chem.* **2014**, *53*, 5893.

DOI: 10.1021/jacs.5b00816
J. Am. Chem. Soc. 2015, 137, 4614−4617